

## Ferromagnetism in LaCoO<sub>3</sub> nanoparticles

Shiming Zhou, Lei Shi,\* Jiyin Zhao, Laifa He, Haipeng Yang, and Shangming Zhang

*Hefei National Laboratory for Physical Sciences at Microscale, University of Science and Technology of China, Hefei, Anhui 230026, People's Republic of China*

(Received 8 May 2007; revised manuscript received 8 July 2007; published 12 November 2007)

We have investigated the structural and magnetic properties of LaCoO<sub>3</sub> nanoparticles prepared by a sol-gel method. A ferromagnetic order with  $T_C \sim 85$  K has been observed in the nanoparticles. The infrared spectra give evidence for a stabilizing of higher spin state and a reduced Jahn-Teller distortion in the nanoparticles with respect to the bulk LaCoO<sub>3</sub>, which is consistent with the recent reports in the strained films [Phys. Rev. B **75**, 144402 (2007)] and proposed to be the possible origin of the observed ferromagnetic order in LaCoO<sub>3</sub>.

DOI: [10.1103/PhysRevB.76.172407](https://doi.org/10.1103/PhysRevB.76.172407)

PACS number(s): 75.60.Ej, 78.30.-j, 75.50.Tt

### I. INTRODUCTION

Due to its thermally induced spin-state and semiconductor-metal transitions, LaCoO<sub>3</sub> has attracted much interest and attention. The electron configuration of Co<sup>3+</sup> ions in LaCoO<sub>3</sub> is  $3d^6$ . At low temperature, since the crystal-field splitting  $\Delta_{CF}$  exceeds the intra-atomic exchange interaction (Hund's rule coupling) energy  $J_{ex}$ , all electrons occupy the  $t_{2g}$  level, giving a nonmagnetic low-spin (LS) ( $t_{2g}^6 e_g^0$ ,  $S=0$ ) ground state. As the temperature increases, LaCoO<sub>3</sub> undergoes a transition from nonmagnetic to paramagnetic state evidenced by an abnormally steep increase of the magnetic susceptibility between 35 and 100 K, and a gradual semiconductor-metal transition accompanied by another broad anomaly in the magnetic susceptibility around 500 K. The two anomalies are usually ascribed to thermally activated spin-state transitions. The classic explanation invoked the appearance of the high-spin (HS) ( $t_{2g}^4 e_g^2$ ,  $S=2$ ) state of Co<sup>3+</sup>.<sup>1</sup> However, the failure to observe any superstructure expected for this framework in neutron diffraction studies was incompatible with the simple LS-HS model.<sup>2</sup> Later, a completely different description including the formation of an intermediate spin (IS) ( $t_{2g}^5 e_g^1$ ,  $S=1$ ) was proposed<sup>3</sup> and supported by the local density approximation plus Hubbard calculations.<sup>4</sup> In this framework, the first anomaly around 100 K is associated with the LS-IS transition, whereas the second one around 500 K corresponds to a transition from the IS state to a mixed state of IS and HS. This three-level LS-IS-HS model has been successfully applied to interpret the results of numerous different experiments<sup>5-12</sup> and has become the most widely accepted framework for the transitions in LaCoO<sub>3</sub>. However, very recently, in the studies of inelastic neutron scattering,<sup>13</sup> soft x-ray absorption spectroscopy, and magnetic circular dichroism,<sup>14</sup> the IS state has been questioned and the HS state has been reinvented. Those conflicting interpretations mean that further studies are required to define the precise spin states in this compound.

Despite the nonmagnetic LS ground state, there are two interesting but puzzling magnetic behaviors at low temperature in LaCoO<sub>3</sub>. One is a Curie-Weiss paramagnetic component in the low temperature magnetic susceptibility (below 35 K), which is usually reported in LaCoO<sub>3</sub>. The component was previously ascribed to impurities<sup>5</sup> or to localized spins associated with the surface and/or lattice defects.<sup>1</sup> It is

unlikely due to substitutional impurities or lattice defects since they are found by all investigators on both polycrystalline and single-crystal samples. Recently, Yan *et al.*<sup>15</sup> observed the presence of a similar behavior also in PrCoO<sub>3</sub> and NdCoO<sub>3</sub> at relatively higher temperatures and suggested that the behavior should be intrinsic properties arising from surface cobalt, possibly a LS ground state bearing some IS character caused by virtual excitation to the IS state.

The more surprising and confusing one is the existence of either long- or short-range ferromagnetic order reported in some literatures.<sup>16-19</sup> Earlier, Menyuk *et al.*<sup>16</sup> reported a hysteresis in the magnetization of LaCoO<sub>3</sub> at 1.9 K in both precipitated powders and a ground single crystal and attributed it to the presence of small isolated magnetic regions dispersed in nonmagnetic matrix. Recently, Androulakis *et al.*<sup>17</sup> revealed two ferromagnetic phases, one with  $T_C < 10$  K and the other with  $20 \text{ K} < T_C < 100 \text{ K}$ , in coprecipitation derived LaCoO<sub>3</sub> powders and ascribed them to the presence of Co<sup>4+</sup> ions due to La<sup>3+</sup> vacancies. Yan *et al.*<sup>18</sup> observed a ferromagnetic component with  $T_C \sim 85$  K in ground single crystals. They found an increase of remanence and coercivity with the increase of surface/volume ratio of the different samples and excluded the ferromagnetic coupling by oxidized clusters due to the low value of  $T_C$ . The coordination of surface Co<sup>3+</sup> ions was argued to be capable of stabilizing higher spin state, most probably an IS state, and a ferromagnetic coupling between higher-spin Co<sup>3+</sup> ions was proposed. In a very recent work, Fuchs *et al.*<sup>19</sup> reported that a similar ferromagnetic order is also present in epitaxially strained thin films and disclosed a linear increase of the saturated magnetic moment with increasing film thickness, which proves the ferromagnetism over the complete film thickness. Tensile strain induced by a chosen substrate, but not surface, has been attributed to result in the ferromagnetic order. These conflicting results strongly imply that the origin of the observed ferromagnetism in LaCoO<sub>3</sub> is still an open question. On the other hand, if  $T_C$  is determined from the onset of the field-cooling (FC) magnetization under  $H < 1$  T, we notice that though those studied samples in Refs. 17-19 were prepared by different methods and in much different forms, they have given almost the same value of  $T_C$ ,  $\sim 85$  K, which strongly suggests that the origin of the observed ferromagnetic order may be unique. Of course, to identify it, more experiments on the LaCoO<sub>3</sub> samples with different forms are needed.

In this work, we have investigated the structural and magnetic properties of LaCoO<sub>3</sub> nanoparticles prepared by a sol-

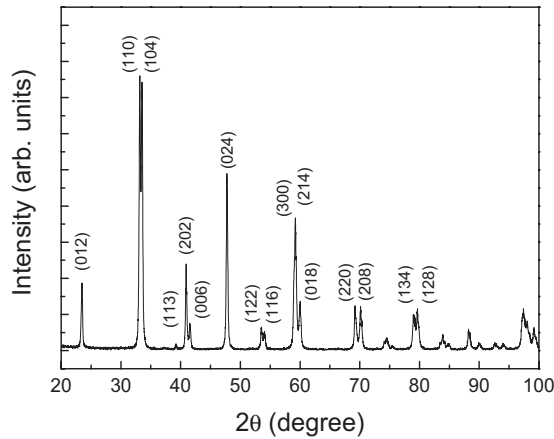


FIG. 1. Room temperature x-ray diffraction pattern of the  $\text{LaCoO}_3$  nanoparticles.

gel method. A ferromagnetic order with  $T_C \sim 85$  K has also been observed in the nanoparticles. The infrared spectroscopy of the nanoparticles gives evidence for a stabilizing higher spin state and reduced Jahn-Teller (JT) distortions in the nanoparticles with respect to the bulk sample. These results are consistent with the reports in the strained film<sup>19</sup> and are proposed to be the possible origin of the observed ferromagnetic order in  $\text{LaCoO}_3$ .

## II. EXPERIMENTAL DETAILS

$\text{LaCoO}_3$  nanoparticles were prepared by a sol-gel method. The gel was decomposed at about  $400^\circ\text{C}$  for 4 h to result a dark brown powder, which was further annealed at  $700^\circ\text{C}$  for 6 h to obtain  $\text{LaCoO}_3$  nanoparticles. For comparison, a  $\text{LaCoO}_3$  bulk sample was also prepared by a conventional solid state reaction. The phase purity and crystal structure of the nanoparticles were determined by an 18 kW rotating anode x-ray diffractometer (XRD) (type MXP18AHF, MAC Science) with graphite monochromatized  $\text{Cu } K_\alpha$  ( $\lambda = 1.5418 \text{ \AA}$ ) radiation in the Bragg-Brentano geometry at room temperature. The particle sizes and morphology were determined by a JEOL (model JSM-6700F) field emission scanning electron microanalyzer (SEM). The measurements of infrared (IR) absorption spectra were recorded with a Nicolet model Magna 750 Fourier transform spectrometer using KBr as a carrier. The magnetic measurements were carried out with a superconducting quantum interference device magnetometer (Quantum Design MPMS XL-7).

## III. RESULTS AND DISCUSSION

The room temperature x-ray diffraction pattern of the  $\text{LaCoO}_3$  nanoparticles is shown in Fig. 1. All diffraction peaks can be indexed by a single phase with rhombohedral crystal structure (space group  $R\bar{3}C$ ), such as the bulk sample (not shown here). The lattice parameters obtained from the pattern are  $a = 5.445(1) \text{ \AA}$  and  $c = 13.109(1) \text{ \AA}$ , which are larger than those of the bulk sample [ $a = 5.442(1) \text{ \AA}$  and  $c = 13.088(1) \text{ \AA}$ ], indicating an expansion of the unit cell in

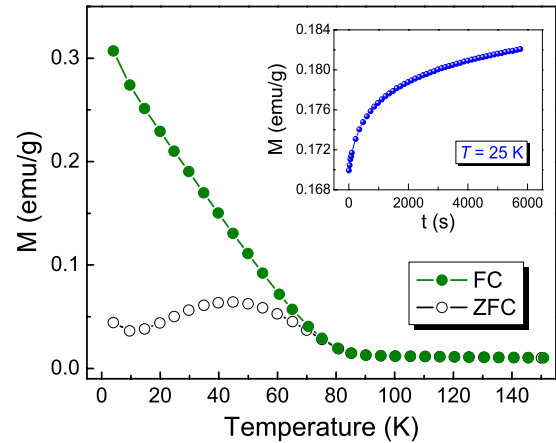


FIG. 2. (Color online) ZFC and FC magnetization measured at  $H = 500$  Oe for the  $\text{LaCoO}_3$  nanoparticles. The inset shows the time dependence of ZFC magnetization measured for  $H = 2$  kOe at 25 K.

the nanoparticles. The crystalline size of the nanoparticles, determined by the Scherrer formula  $D = 0.89\lambda / B \cos \theta$ , where  $\lambda$  is the x-ray wavelength and  $B$  is the full width at half maximum of XRD peaks after an instrumental broadening correction, is about 33 nm. The SEM study (not shown here) reveals the average particle size of  $\sim 80$  nm, implying the possible presence of aggregated particles.

For the bulk  $\text{LaCoO}_3$ , the temperature dependent magnetization below 150 K agrees well with the previous reports.<sup>1,5,6</sup> However, for the nanoparticles, a significant scenario appears. Figure 2 shows the temperature dependence of zero-field-cooling (ZFC) and field-cooling (FC) magnetization for the nanoparticles below 150 K under a field of 500 Oe. The FC curve shows a clear ferromagnetic order below 85 K. The Curie temperature  $T_C$ , determined from the onset of the FC magnetization, is about 85 K, which is very consistent with the reported values in Refs. 17–19. The existence of ferromagnetism below 85 K for the nanoparticles is further confirmed by the observed evident hysteresis loop in the field dependent magnetization, as shown in Fig. 3. No clear hysteresis loop is found at low temperature for the bulk (not shown here), whereas a very evident hysteresis is ob-

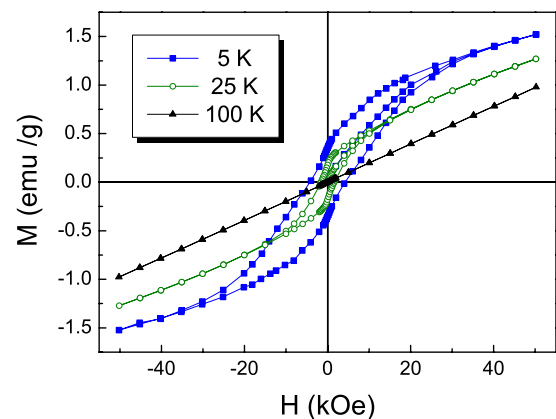


FIG. 3. (Color online) Field dependent magnetization at 5, 25, and 100 K for the  $\text{LaCoO}_3$  nanoparticles.

served below 85 K for the nanoparticles, and the coercivity and remanence are markedly increased as the temperature is lowered. The coercive field is about 1.6 kOe at 25 K, and increases sharply to about 4.3 kOe at 5 K, which is comparable with the reported values of the ground single crystals<sup>18</sup> and strained films<sup>19</sup> at the same temperature.

On the other hand, a large divergence of the FC and ZFC magnetization curves is observed below 80 K. Moreover, the ZFC curve exhibits a cusp at  $\sim 45$  K. The large divergence between the FC and ZFC curves and the cusp in the ZFC curve are usually typical characteristics of a glasslike behavior. To further investigate the magnetic properties of the LaCoO<sub>3</sub> nanoparticles at low temperatures, a ZFC long-time relaxation of magnetization is measured at 25 K with a fixed measuring field of 2 kOe, as shown in the inset of Fig. 2. One can see that the time dependent magnetization does not display any sign of saturation even after 6000 s, indicating the system far from the equilibrium. It is generally believed that the long-time magnetization relaxation should be attributed to the glassy behavior as the measuring field is larger than the coercive field.<sup>20</sup> Since the coercive field at 25 K is smaller than 2 kOe, the relaxation may result from glassy processes. Of course, to identify this system as spin glass or cluster spin glass or others, more studies about ac susceptibility, aging effect, memory effect, and so on should be required, which are beyond the scope of this work.

Above 110 K, the nanoparticles exhibit a paramagnetic state, where the magnetic susceptibility obeys the Curie-Weiss law. The effective paramagnetic moment per Co ion obtained from the susceptibility above 110 K is about  $3.8\mu_B$ , corresponding to a spin state of  $S \approx 1.5$ . This value agrees well with that of the strained films in Ref. 19, which indicates a much stronger occupation of higher spin state. The cobalt ion spin at the surface of LaCoO<sub>3</sub> particles can be stabilized as a higher spin state, possible IS state, due to a reducing oxygen coordination, as discussed in Ref. 18. Since the surface/volume ratio is much large in nanoparticles, the increased population of higher spin states in the LaCoO<sub>3</sub> nanoparticles can be understandable. On the other hand, the higher spin state Co<sup>3+</sup> ions have a larger radius ( $\sim 0.61$  Å for HS and  $\sim 0.56$  Å for IS) than the LS state ( $\sim 0.545$  Å), and the volume expansion has been reported to be accompanied by the spin state transitions from LS to higher spin states.<sup>7</sup> For our nanoparticles, one can see that the stabilization of higher spin state is also associated with the expansion of the unit cell, as observed in our XRD results.

It is well known that in bulk LaCoO<sub>3</sub>, the IS state of Co<sup>3+</sup> ions is expected to be strong JT active due to the partially occupied  $e_g$  orbital and that a cooperative JT distortion causes an orbital ordering. The local JT distortion and orbital ordering had been revealed by many experiments.<sup>5-12</sup> Yamaguchi *et al.*<sup>5</sup> observed an anomalous splitting of the phonon modes as well as their intensity variation with temperature during the spin-state transition in their infrared reflectivity spectra. Three stretching modes ( $S_1$ ,  $S_2$ , and  $S_3$ ) are revealed around  $540$  cm<sup>-1</sup> and are assigned to the vibration of an oxygen atom between Co ions with different spin states: mode  $S_1$  with the medium energy to all the LS-containing bonds, mode  $S_2$  with the high energy, and  $S_3$  with the low energy to two splitting bonds in the orbital-ordered

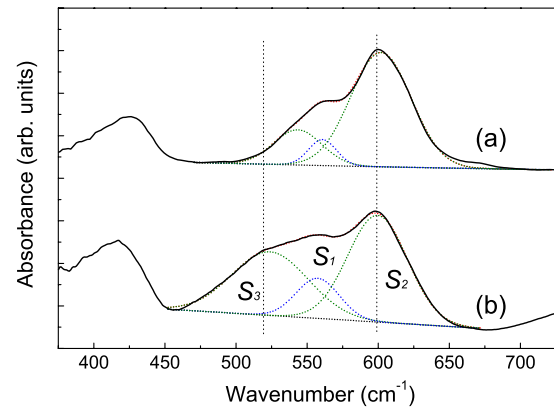


FIG. 4. (Color online) Room temperature IR spectra for the nanoparticles (a) and bulk sample (b) of LaCoO<sub>3</sub>. The dashed lines represent the best-fitted results with three Gaussian lines  $S_1$ ,  $S_2$ , and  $S_3$ .

IS state due to the JT distortion. The splitting of modes  $S_2$  and  $S_3$  at high temperatures reflects the JT effect of the IS Co<sup>3+</sup> ions. Maris *et al.*<sup>8</sup> revealed three unequal Co-O bonds in LaCoO<sub>3</sub> by x-ray diffraction: the short and long ones in the  $ab$  plane and the medium one at the out of plane. The alternation of the short and long bonds indicates the presence of the  $e_g$  orbital ordering induced by a cooperative JT distortion, and the difference between two bonds characterizes the magnitude of JT distortion. Since the stretching modes are related with the Co-O distance, the two studies on the IR spectra and x-ray diffraction can be in agreement with each other. In Ref. 19, the authors suggested that the tensile strain in epitaxial strained LaCoO<sub>3</sub> films results not only in the stabilization of higher spin states but also in the suppression of the JT distortion. The latter was proposed to reduce the splitting of the  $e_g$  orbitals, which will lead the orbitals to favor ferromagnetic superexchange<sup>21</sup> and give rise to the observed ferromagnetic order. As discussed in the Introduction, the origins of the ferromagnetism observed in LaCoO<sub>3</sub> with different forms may be the same. Thus, we presume that the splitting of the  $e_g$  orbitals should be reduced in our nanoparticles. Since the IR spectroscopy is a sensitive tool to probe the local lattice changes,<sup>5</sup> it has been carried out on the nanoparticles and the bulk sample of LaCoO<sub>3</sub> to confirm our hypothesis.

Figure 4 shows the room temperature IR absorption spectra for the nanoparticles and bulk sample, where two bands are found at around  $600$  and  $420$  cm<sup>-1</sup>. The former is usually attributed to the stretching mode<sup>5,22</sup> and the latter to the Brillouin-zone-folded<sup>5</sup> or bending<sup>22</sup> mode. Since the stretching modes are related to the Co-O bonds, we only focus on the stretching modes here. Three Gaussian lines, corresponding to the three modes  $S_1$ ,  $S_2$ , and  $S_3$ , have been used to fit the observed spectra for both samples, as shown in Fig. 4. For the bulk sample, the relative intensity of mode  $S_1$ , determined from the area of mode  $S_1$  normalized to the total area of three modes and proposed to approximately represent the occupied population of the LS state according to Ref. 5, is about 13%, which is consistent with the result from the Raman scattering,<sup>9</sup> where the occupancy of the IS state was

reported to be about 84% at 300 K. The splitting between modes  $S_2$  and  $S_3$ , which characterizes the magnitude of JT distortion, is  $\sim 75.6 \text{ cm}^{-1}$ . However, compared to the bulk, the nanoparticles display two distinct changes in the stretching modes. First, the relative intensity of mode  $S_1$  decreases to  $\sim 7\%$ . This decrease points out a loss of the LS state in the  $\text{LaCoO}_3$  nanoparticles. In other words, an increased population of higher spin states, most possibly IS state, is present for the nanoparticles with respect to the bulk, which is consistent with the XRD results and magnetic properties discussed above. Second, the splitting between modes  $S_2$  and  $S_3$  remarkably decreases to  $\sim 58.7 \text{ cm}^{-1}$ , which strongly indicates that the JT distortion is significantly reduced in the  $\text{LaCoO}_3$  nanoparticles. Since the reduction of the JT distortion will weaken the splitting of the  $e_g$  orbitals, the IR spectra clearly confirm our hypothesis. The two distinct changes in the IR spectra provide evidence for the stabilization of higher spin states and the decrease of the splitting of the  $e_g$  orbitals in the  $\text{LaCoO}_3$  nanoparticles with respect to the bulk, which agree quite well with those reported in strained  $\text{LaCoO}_3$

films<sup>19</sup> and are proposed to be the possible origin of the observed ferromagnetism in  $\text{LaCoO}_3$ .

#### IV. CONCLUSION

The structural and magnetic properties of  $\text{LaCoO}_3$  nanoparticles have been investigated. A ferromagnetic order with  $T_C$  of  $\sim 85 \text{ K}$  is found. The IR spectra reveal two distinct features in the nanoparticles with respect to the bulk  $\text{LaCoO}_3$ . One is an increased population of higher spin state and the other is a reduced splitting of the  $e_g$  orbitals, which are in good agreement with the recent reports in the strained films and are considered as the possible origin of the observed ferromagnetism in  $\text{LaCoO}_3$ .

#### ACKNOWLEDGMENTS

This project was financially supported by the Ministry of Science and Technology of China (NKBRFSF-G1999064603), and the National Science Foundation of China (Grant No. 10174071).

\*Author to whom correspondence should be addressed; shil@ustc.edu.cn

<sup>1</sup>J. B. Goodenough, *Prog. Solid State Chem.* **5**, 145 (1971); M. A. Señarís-Rodríguez and J. B. Goodenough, *J. Solid State Chem.* **116**, 224 (1995).

<sup>2</sup>G. Thornton, B. C. Tofield, and A. W. Hewat, *J. Solid State Chem.* **61**, 301 (1986).

<sup>3</sup>R. H. Potze, G. A. Sawatzky, and M. Abbate, *Phys. Rev. B* **51**, 11501 (1995).

<sup>4</sup>M. A. Korotin, S. Yu. Ezhov, I. V. Solovyev, V. I. Anisimov, D. I. Khomskii, and G. A. Sawatzky, *Phys. Rev. B* **54**, 5309 (1996).

<sup>5</sup>S. Yamaguchi, Y. Okimoto, and Y. Tokura, *Phys. Rev. B* **55**, R8666 (1997).

<sup>6</sup>C. Zobel, M. Kriener, D. Bruns, J. Baier, M. Grüninger, T. Lorenz, P. Reutler, and A. Revcolevschi, *Phys. Rev. B* **66**, 020402(R) (2002).

<sup>7</sup>P. G. Radaelli and S.-W. Cheong, *Phys. Rev. B* **66**, 094408 (2002).

<sup>8</sup>G. Maris, Y. Ren, V. Volotchaev, C. Zobel, T. Lorenz, and T. T. M. Palstra, *Phys. Rev. B* **67**, 224423 (2003).

<sup>9</sup>A. Ishikawa, J. Nohara, and S. Sugai, *Phys. Rev. Lett.* **93**, 136401 (2004).

<sup>10</sup>J. Baier, S. Jodlauk, M. Kriener, A. Reichl, C. Zobel, H. Kierspel, A. Freimuth, and T. Lorenz, *Phys. Rev. B* **71**, 014443 (2005).

<sup>11</sup>M. Medarde, C. Dallera, M. Grioni, J. Voigt, A. Podlesnyak, E. Pomjakushina, K. Conder, Th. Neisius, O. Tjénberg, and S. N.

Barilo, *Phys. Rev. B* **73**, 054424 (2006).

<sup>12</sup>D. Phelan, D. Louca, S. Rosenkranz, S.-H. Lee, Y. Qiu, P. J. Chupas, R. Osborn, H. Zheng, J. F. Mitchell, J. R. D. Copley, J. L. Sarrão, and Y. Moritomo, *Phys. Rev. Lett.* **96**, 027201 (2006).

<sup>13</sup>A. Podlesnyak, S. Streule, J. Mesot, M. Medarde, E. Pomjakushina, K. Conder, A. Tanaka, M. W. Haverkort, and D. I. Khomskii, *Phys. Rev. Lett.* **97**, 247208 (2006).

<sup>14</sup>M. W. Haverkort, Z. Hu, J. C. Cezar, T. Burnus, H. Hartmann, M. Reuther, C. Zobel, T. Lorenz, A. Tanaka, N. B. Brookes, H. H. Hsieh, H.-J. Lin, C. T. Chen, and L. H. Tjeng, *Phys. Rev. Lett.* **97**, 176405 (2006).

<sup>15</sup>J.-Q. Yan, J. S. Zhou, and J. B. Goodenough, *Phys. Rev. B* **69**, 134409 (2004).

<sup>16</sup>Menyuk, K. Dwight, and P. M. Raccach, *J. Phys. Chem. Solids* **28**, 549 (1967).

<sup>17</sup>J. Androulakis, N. Katsarakis, and J. Giapintzakis, *Phys. Rev. B* **64**, 174401 (2001).

<sup>18</sup>J.-Q. Yan, J. S. Zhou, and J. B. Goodenough, *Phys. Rev. B* **70**, 014402 (2004).

<sup>19</sup>D. Fuchs, C. Pinta, T. Schwarz, P. Schweiss, P. Nagel, S. Schuppler, R. Schneider, M. Merz, G. Roth, and H. Löhneysen, *Phys. Rev. B* **75**, 144402 (2007).

<sup>20</sup>K. Binder and A. P. Young, *Rev. Mod. Phys.* **58**, 801 (1986).

<sup>21</sup>T. Mizokawa and A. Fujimori, *Phys. Rev. B* **51**, 12880 (1995).

<sup>22</sup>L. Sudheendra, Md. Motin Seikh, A. R. Raju, and Chandrabhas Narayana, *Chem. Phys. Lett.* **340**, 275 (2001).